Logically Rectangular Mixed Methods for Groundwater Flow and Transport on General Geometry

Todd Arbogast

Mary F. Wheeler

Ivan Yotov

CRPC-TR94376

January, 1994

Revised June, 1994.

LOGICALLY RECTANGULAR MIXED METHODS FOR GROUNDWATER FLOW AND TRANSPORT ON GENERAL GEOMETRY

TODD ARBOGAST, MARY F. WHEELER, and IVAN YOTOV

Department of Computational and Applied Mathematics
Rice University
Houston, Texas 77251–1892
U.S.A.

ABSTRACT

We consider an extended mixed finite element formulation for groundwater flow and transport problems with either a tensor hydraulic conductivity or a tensor dispersion. While the aquifer domain can be geometrically general, in our formulation the computational domain is rectangular. The approximating spaces for the mixed method are defined on a smooth curvilinear grid, obtained by a global mapping of the rectangular, computational grid. The original problem is mapped to the computational domain, giving a similar problem with a modified tensor coefficient. Special quadrature rules are introduced to transform the mixed method into a simple cell-centered finite difference method with a 9 point stencil in 2-D and 19 point stencil in 3-D. The resulting scheme is locally mass conservative. In the case of flow, linear Galerkin procedures give first order accurate velocities, while our method is second order accurate. Both computational and theoretical results are given.

1. INTRODUCTION

We develop a numerical scheme for groundwater flow and transport problems with tensor coefficients on a geometrically general domain Ω in $\mathbf{R}^d$ ($d = 2$ or 3). In the flow problem, we solve for the pressure p and the velocity $\mathbf{u}$ satisfying

$$(1.1) \qquad \nabla \cdot \mathbf{u} = q, \quad \mathbf{u} = -K\nabla p,$$

where K is the hydraulic conductivity tensor. In the transport problem, we solve for the concentration c such that

$$(1.2) \qquad \phi\frac{\partial c}{\partial t} + \nabla \cdot \big(\mathbf{u}c - D(\mathbf{u})\nabla c\big) = q_c(c),$$

where ϕ is the porosity and D is the dispersion tensor with components

$$(1.3) \qquad D_{i,j}(\mathbf{u}) = \phi d_m \delta_{i,j} + |\mathbf{u}|\left\{\frac{u_i u_j}{|\mathbf{u}|^2}(d_l - d_t) + d_t\delta_{i,j}\right\},$$

where d_m is the molecular diffusivity and d_l, and d_t are the longitudinal and transverse dispersivity, respectively. For simplicity of the presentation, we consider homogeneous Neumann boundary conditions.

Our numerical scheme is based on mixed finite element methods, because they conserve mass locally and give a good approximation of the flux variable. However, mixed methods can be difficult to implement directly.

By using special quadrature rules for evaluating the integrals, Russell and Wheeler [6] showed that the standard cell-centered finite difference method was equivalent to the lowest order, RT_0 mixed method [5]. Thus, the RT_0 mixed method can be easily implemented as a five or seven point finite difference method. Weiser and Wheeler [8] obtained superconvergence results for this scheme; that is, if h is the maximum grid spacing, both the pressure and velocity are approximated to order h^2. A Galerkin method will approximate the velocity only to order h.

Those two works were limited to the case of a diagonal tensor and a rectangular grid. To solve our flow and transport problems with tensor coefficients on fairly geometrically general domains, we develop a new scheme to overcome these limitations. We will not sacrifice the ease of implementation, the accuracy, or the local mass conservation property of the approximation. In the notation of the flow problem, we present in the next section some of the necessary background of the expanded mixed finite element method that is the basis of our scheme [4]. We derive our finite difference procedure [3] from it in Section 3. We summarize the convergence results [4] in Section 4. Transport is discussed briefly in Section 5, and computational results are given in Section 6.

Our main requirement is that there be a smooth mapping F of a rectangular, computational domain $\hat{\Omega}$ onto the aquifer domain Ω. Given a rectangular grid $\hat{\mathcal{T}}_h$ on $\hat{\Omega}$, F defines a smooth, logically rectangular, curvilinear grid $\mathcal{T}_h$ on Ω (see Fig. 1). The Jacobian matrix of F is $DF = \left(\partial F_i/\partial x_j\right)$, and the Jacobian of the mapping is $J = |\det(DF)|$. (There are grid generation codes available for creating F and its Jacobian matrix.)
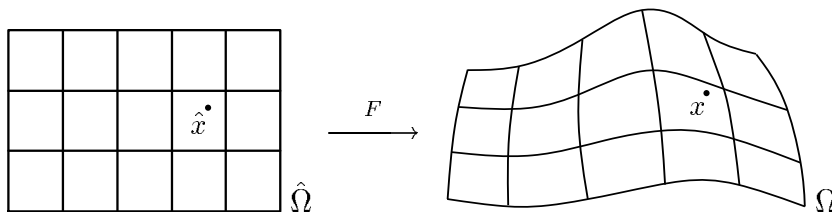

Fig. 1. The computational domain $\hat{\Omega}$ and the physical domain Ω.

2. THE EXPANDED MIXED FINITE ELEMENT METHOD ON GENERAL GEOMETRY

Following [3] and [4], we introduce an unknown $\tilde{\mathbf{u}}$ such that

$$(2.1) \qquad M\tilde{\mathbf{u}} = -\nabla p, \quad \mathbf{u} = KM\tilde{\mathbf{u}},$$

where $M = J(DF^{-1})^T DF^{-1}$. Note that M is a symmetric, positive definite matrix. It is introduced to simplify the computations significantly, after mapping to the rectangular grid on $\hat{\Omega}$.

To define the RT_0 mixed space on the curvilinear grid, we need first the standard definition of this space on rectangles [5]. Let $\hat{V}_h$ and $\hat{W}_h$ be the velocity and the pressure space, respectively. On any rectangular element $\hat{E} \in \hat{\mathcal{T}}_h$,

$$\hat{V}_h(\hat{E}) = \left\{ (\alpha_1 x_1 + \beta_1, \alpha_2 x_2 + \beta_2, \alpha_3 x_3 + \beta_3)^T : \alpha_i, \beta_i \in \mathbf{R} \right\},$$
$$\hat{W}_h(\hat{E}) = \left\{ \alpha : \alpha \in \mathbf{R} \right\}$$

(where the last component in $\hat{V}_h(\hat{E})$ should be deleted if $d = 2$). Then,

$$\hat{V}_h = \left\{ \hat{\mathbf{v}} = (v_1, v_2, v_3) : \hat{\mathbf{v}}|_{\hat{E}} \in \hat{V}_h(\hat{E}) \text{ for all } \hat{E} \in \hat{\mathcal{T}}_h, \text{ and each } v_i \text{ is} \right.$$
$$\left. \text{continuous in the } i\text{th coordinate direction} \right\},$$
$$\hat{W}_h = \left\{ \hat{w} : \hat{w}|_{\hat{E}} \in \hat{W}_h(\hat{E}) \text{ for all } \hat{E} \in \hat{\mathcal{T}}_h \right\};$$

thus, if $\hat{\nu}$ denotes the normal direction, $\hat{\mathbf{v}} \cdot \hat{\nu}$ is well defined on the boundaries of each element $\hat{E}$, and $\hat{w}$ is piecewise discontinuous. We use the standard nodal basis, where for $\hat{V}_h$, the nodes are at the midpoints of the edges or faces of the elements, and for $\hat{W}_h$, the nodes are at the midpoints of the elements (cell-centers).

Let V_h and W_h be the RT_0 spaces on $\mathcal{T}_h$, defined as follows [7]. For each $\hat{\mathbf{v}} \in \hat{V}_h$ and $\hat{w} \in \hat{W}_h$, we define $\mathbf{v} \in V_h$ and $w \in W_h$ at $F(\hat{x}) = x \in \Omega$ by

(2.2a) $$\mathbf{v}(x) = \frac{1}{J(\hat{x})} DF(\hat{x}) \hat{\mathbf{v}}(\hat{x}),$$

(2.2b) $$w(x) = \hat{w}(\hat{x}).$$

The velocity space is defined by the Piola transformation; it preserves the normal component of the velocity across the element boundaries, and is therefore locally mass conservative. The key property is that $\nabla \cdot \mathbf{v} = \frac{1}{J} \hat{\nabla} \cdot \hat{\mathbf{v}}$.

We have the following mixed formulation for approximating the flow equation (1.1). Find $\mathbf{u}_h \in V_h$, $\tilde{\mathbf{u}}_h \in V_h$, and $p_h \in W_h$ such that

(2.3a) $$\int_E \nabla \cdot \mathbf{u}_h \, dx = \int_E q \, dx, \qquad E \in \mathcal{T}_h,$$

(2.3b) $$\int_\Omega M \tilde{\mathbf{u}}_h \cdot \mathbf{v} \, dx = \int_\Omega p_h \nabla \cdot \mathbf{v} \, dx, \qquad \mathbf{v} \in V_h,$$

(2.3c) $$\int_\Omega M \mathbf{u}_h \cdot \mathbf{v} \, dx = \int_\Omega M K M \tilde{\mathbf{u}}_h \cdot \mathbf{v} \, dx, \quad \mathbf{v} \in V_h.$$

The existence and uniqueness of a solution is shown in [4].

We now transform (2.3) to the rectangular, computational domain by the map F. The Piola transform (2.2a), (2.2b), and the definition of M (2.1) imply that

$$(2.4a) \qquad \int_{\hat{E}} \hat{\nabla} \cdot \hat{\mathbf{u}}_h \, d\hat{x} = \int_E q \, dx = \int_{\hat{E}} \hat{q} J \, d\hat{x}, \qquad \hat{E} \in \hat{\mathcal{T}}_h,$$

$$(2.4b) \qquad \int_{\hat{\Omega}} \hat{\mathbf{u}}_h \cdot \hat{\mathbf{v}} \, d\hat{x} = \int_{\hat{\Omega}} \hat{p}_h \hat{\nabla} \cdot \hat{\mathbf{v}} \, d\hat{x}, \qquad \hat{\mathbf{v}} \in \hat{V}_h,$$

$$(2.4c) \qquad \int_{\hat{\Omega}} \hat{\mathbf{u}}_h \cdot \hat{\mathbf{v}} \, d\hat{x} = \int_{\hat{\Omega}} J DF^{-1} K (DF^{-1})^T \tilde{\hat{\mathbf{u}}}_h \cdot \hat{\mathbf{v}} \, d\hat{x}, \quad \hat{\mathbf{v}} \in \hat{V}_h,$$

where $\hat{q}(\hat{x}) = q(F(\hat{x}))$. Note that (2.4) is similar to the original problem (2.3) with $M = I$ and the modified tensor coefficient

$$(2.5) \qquad \qquad \mathcal{K} = J DF^{-1} K (DF^{-1})^T.$$

All computations are performed on the rectangular grid of $\hat{\Omega}$; we recover the true pressure and velocity on Ω using (2.2).

3. THE CELL-CENTERED FINITE DIFFERENCE METHOD

To simplify the finite element method (2.4), we use special quadrature rules for approximating the integrals. The two divergence integrals can be computed exactly, since the divergence of any $\hat{\mathbf{v}} \in \hat{V}_h$ is piece-wise constant. The trapezoidal rule is used for evaluating the three integrals involving a vector-vector product. This enables us to express $\hat{\mathbf{u}}_h$ and $\tilde{\hat{\mathbf{u}}}_h$ in terms of $\hat{p}_h$, and therefore obtain a single equation for the pressure. Herein, we describe this stencil for $d = 2$; a straightforward generalization gives the stencil for $d = 3$.

We need some relatively standard cell-centered finite difference notation. Denote the grid points by

$$(\hat{x}_{i+1/2}, \hat{y}_{j+1/2}), \quad i = 0, ..., N_1, \; j = 0, ..., N_2,$$

and define, for $i = 1, ..., N_1$ and $j = 1, ..., N_2$,

$$\hat{x}_i = \tfrac{1}{2}(\hat{x}_{i+1/2} + \hat{x}_{i-1/2}), \qquad \hat{y}_j = \tfrac{1}{2}(\hat{y}_{j+1/2} + \hat{y}_{j-1/2}),$$

$$\hat{h}_i^{\hat{x}} = \hat{x}_{i+1/2} - \hat{x}_{i-1/2}, \qquad \hat{h}_j^{\hat{y}} = \hat{y}_{j+1/2} - \hat{y}_{j-1/2}.$$

We write $\mathbf{v} = (v^{\hat{x}}, v^{\hat{y}})$ for $\mathbf{v} \in \mathbf{R}^2$, and for any function $g(\hat{x}, \hat{y})$, let g_{ij} denote $g(\hat{x}_i, \hat{y}_j)$, let $g_{i+1/2, j}$ denote $g(\hat{x}_{i+1/2}, \hat{y}_j)$, etc.

If $\hat{\mathbf{v}}$ in (2.4b) is the basis function at node $(i + 1/2, j)$ or at node $(i, j + 1/2)$, then

$$(3.1) \qquad \tilde{\hat{u}}_{h, i+1/2, j}^{\hat{x}} = -\frac{\hat{p}_{h, i+1, j} - \hat{p}_{h, i, j}}{\frac{1}{2}(\hat{h}_i^{\hat{x}} + \hat{h}_{i+1}^{\hat{x}})}, \qquad \tilde{\hat{u}}_{h, i, j+1/2}^{\hat{y}} = -\frac{\hat{p}_{h, i, j+1} - \hat{p}_{h, i, j}}{\frac{1}{2}(\hat{h}_j^{\hat{y}} + \hat{h}_{j+1}^{\hat{y}})},$$

which is a finite difference approximation of $\hat{\tilde{\mathbf{u}}} = -\hat{\nabla}\hat{p}$. The same choice of $\hat{\mathbf{v}}$ in (2.4c) gives

$$(3.2) \qquad \hat{u}^{\hat{x}}_{h,i+1/2,j} = \frac{1}{2}\left[(\mathcal{K}_{11})_{i+1/2,j-1/2} + (\mathcal{K}_{11})_{i+1/2,j+1/2}\right]\hat{\tilde{u}}^{\hat{x}}_{h,i+1/2,j}$$

$$+ \frac{1}{2(\hat{h}^{\hat{x}}_i + \hat{h}^{\hat{x}}_{i+1})}\Bigg\{$$

$$\left[(\mathcal{K}_{12})_{i+1/2,j-1/2}\hat{\tilde{u}}^{\hat{y}}_{h,i+1,j-1/2} + (\mathcal{K}_{12})_{i+1/2,j+1/2}\hat{\tilde{u}}^{\hat{y}}_{h,i+1,j+1/2}\right]\hat{h}^{\hat{x}}_{i+1}$$

$$+ \left[(\mathcal{K}_{12})_{i+1/2,j-1/2}\hat{\tilde{u}}^{\hat{y}}_{h,i,j-1/2} + (\mathcal{K}_{12})_{i+1/2,j+1/2}\hat{\tilde{u}}^{\hat{y}}_{h,i,j+1/2}\right]\hat{h}^{\hat{x}}_i\Bigg\},$$

with a similar expression for $\hat{u}^{\hat{y}}_{h,i,j+1/2}$; this is a finite difference approximation of $\hat{\mathbf{u}} = \mathcal{K}\hat{\tilde{\mathbf{u}}}$. Finally, for $E = E_{ij}$ in (2.4a), we have

$$(3.3) \qquad \left\{\frac{\hat{u}^{\hat{x}}_{h,i+1/2,j} - \hat{u}^{\hat{x}}_{h,i-1/2,j}}{\hat{h}^{\hat{x}}_i} + \frac{\hat{u}^{\hat{y}}_{h,i,j+1/2} - \hat{u}^{\hat{y}}_{h,i,j-1/2}}{\hat{h}^{\hat{y}}_j}\right\}\hat{h}^{\hat{x}}_i\hat{h}^{\hat{y}}_j$$

$$= \int_{\hat{E}_{ij}} \hat{q}J\,d\hat{x} = \int_{E_{ij}} q\,dx.$$

The combination of (3.1), (3.2), and (3.3) gives our finite difference stencil for the pressure, approximating the elliptic equation $-\hat{\nabla}\cdot\mathcal{K}\hat{\nabla}\hat{p} = \hat{q}J$. This in turn is an approximation of the original problem (1.1). The stencil is 9 points in two dimensions and 19 points in three dimensions.

4. A SUMMARY OF THE CONVERGENCE RESULTS

Let $\|\cdot\|$ denote the L^2-norm; that is, for a scalar or vector function φ,

$$\|\varphi\| = \sqrt{\int_\Omega |\varphi(x)|^2\,dx}.$$

Let $\|\|\cdot\|\|_M$ and $\|\|\cdot\|\|_T$ denote the L^2-norm approximated, respectively, by the midpoint and trapezoidal quadrature rules over our mesh on Ω defined either directly or as induced by F from the computational domain. The proof of the following theorem is given in [4].

Theorem. *There exists a constant C depending on the smoothness of F and the solution, but independent of the maximum grid spacing h, such that*

$$\|\mathbf{u} - \mathbf{u}_h\| + \|\tilde{\mathbf{u}} - \tilde{\mathbf{u}}_h\| \le Ch, \qquad \|\|\mathbf{u} - \mathbf{u}_h\|\|_T + \|\|\tilde{\mathbf{u}} - \tilde{\mathbf{u}}_h\|\|_T \le Ch^2,$$

$$\|p - p_h\| \le Ch, \qquad\qquad \|\|p - p_h\|\|_M \le Ch^2,$$

$$\|\nabla\cdot(\mathbf{u} - \mathbf{u}_h)\| \le Ch.$$

This theorem implies optimal order convergence in the L^2-norms, and, moreover, superconvergence in L^2 for the computed pressure at the cell-centers, and for the computed velocity at the grid points. Furthermore, the normal component of the flux at the midpoints of the edges or faces is also superconvergent (see [4]).

5. TRANSPORT BY THE CHARACTERISTICS-MIXED METHOD

The characteristics-mixed method of Arbogast and Wheeler [1], [2] is a method for approximating the transport problem (1.2)–(1.3). It treats the advection terms $\phi(\partial c/\partial t) + \mathbf{u} \cdot \nabla c$ in (1.2) as a characteristic derivative; that is, essentially (1.2) is viewed as

$$\phi \frac{\partial c}{\partial \tau} - \nabla \cdot D(\mathbf{u})\nabla c = q_c(c) - qc,$$

where τ is the characteristic direction. The characteristics are the solution to

$$\frac{d\check{x}}{dt} = \frac{\mathbf{u}(\check{x}, t)}{\phi(\check{x})}$$

on the physical domain Ω, or after the change of variables,

$$(5.1) \qquad \frac{d\check{\hat{x}}}{dt} = \frac{\hat{\mathbf{u}}(\check{\hat{x}}, t)}{J(\check{\hat{x}})\phi(F(\check{\hat{x}}))}$$

on the computational domain $\hat{\Omega}$; thus, only a factor of J enters into the computation of the characteristics.

The dispersion term, $-\nabla \cdot D(\mathbf{u})\nabla c$, is then treated by a mixed method, as in the case for flow. The dispersion tensor D is a function of the true velocity. It can be expressed on the computational grid by the analogue of (2.5) in terms of $\mathbf{u}$, or in terms of $\hat{\mathbf{u}}$ as

$$(5.2) \qquad \mathcal{D}_{i,j}(\hat{\mathbf{u}}) = J\phi d_m \delta_{i,j} + |DF\hat{\mathbf{u}}|\left\{ \frac{\hat{u}_i \hat{u}_j}{|DF\hat{\mathbf{u}}|^2}(d_l - d_t) + d_t \delta_{i,j} \right\},$$

where $\hat{\phi}(\hat{x}) = \phi(F(\hat{x}))$. There is a small change in the way the speed times J, $|DF\hat{\mathbf{u}}|$, needs to be calculated, and J multiplies $\hat{\phi}$. The other, nondispersion terms are treated on the computational grid after multiplying by the Jacobian factor J.

6. SOME COMPUTATIONAL RESULTS

Tests show that the predicted rates of convergence are obtained by the method, including the superconvergence [3], [4]. The only requirement is that the map F be reasonably smooth; otherwise, there is a degeneration in the convergence rate.

We now present some results of a code that uses the finite difference scheme presented in this paper to solve the coupled flow and transport equations (1.1)–(1.3). The characteristics-mixed method [1], [2] is used for transport. The code is designed to run on a massively parallel, distributed memory computer.

We present first a 2-D example on a circular domain with a single well at the center injecting a tracer solute. Porosity and permeability are uniform; thus, the true solution is radially symmetric. We set the dispersion to zero in this example. Fig. 2A–B show concentration fronts at six equally spaced times. Fig. 2A shows the solution as it appears on the square computational domain. Fig. 2B shows the solution after mapping back to the true domain according to (2.2b). As one can see, the solution on the computational domain is distorted just enough to give concentric circles on the true domain. The radii of these circles increase at the expected rate as measured by the volume swept. Fig. 2C shows the curvilinear grid on the true domain that results from mapping the uniform computational grid.

A. Solution on the   B. Solution on the   C. The curvilinear grid
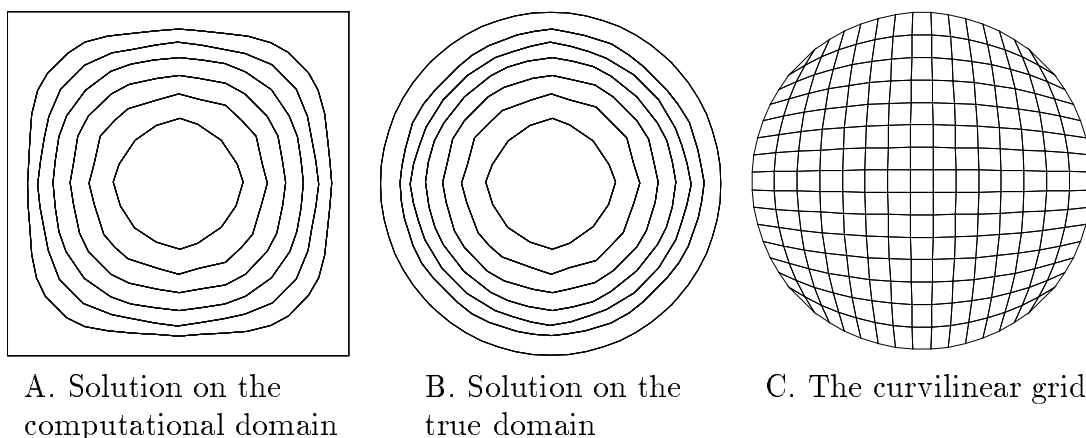computational domain   true domain

Fig. 2. A single injection well at the center of a circular domain.
The solution shows concentration fronts at six equally spaced times.

In Fig. 3, we demonstrate tracer injection at the WAG–6 (Waste Area Grouping #6) site of the Oak Ridge National Laboratory (ORNL). Porosity and permeability are again uniform. A uniform pressure drop occurs from the left face (Haw Ridge) to the right face (White Oak Lake and Copper ridge); there is no-flow across the other faces. Tracer injection occurs at the left face. We show the surface topography and the concentration front at four equally spaced times. The peak of Haw ridge is at the left corner; thus, fluid flow is slower there.
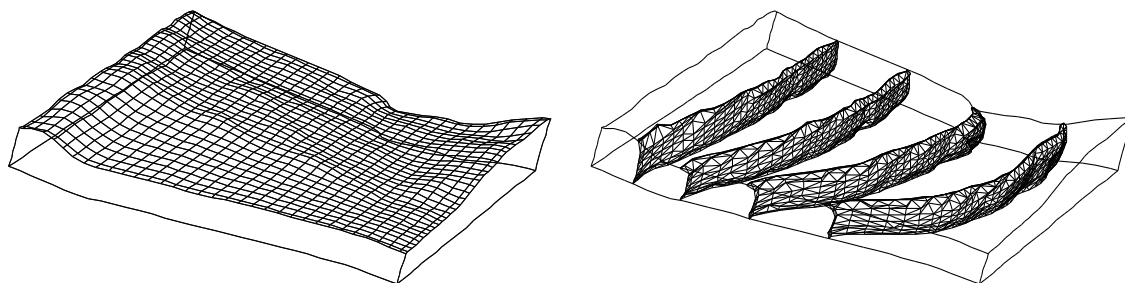

Fig. 3. A demonstration of tracer injection at ORNL WAG–6.

7. CONCLUSIONS

We presented a cell-centered finite difference mixed method that is locally mass conservative and highly accurate, especially for the velocity. General geometry can be handled by a mapping of a rectangular, computational domain to the physical domain. The net result of this mapping is a simple transformation of the tensor conductivity or dispersivity, and possibly the multiplication of certain other coefficients by the Jacobian factor. The scheme is easily implemented, since the data structures need only reflect the rectangular, computational grid.

REFERENCES

[1] Arbogast, T., Chilakapati, A., and Wheeler, M.F. (1992) "A characteristic-mixed method for contaminant transport and miscible displacement", in Russell, Ewing, Brebbia, Gray, and Pindar (eds.), Computational Methods in Water Resources IX, Vol. 1: Numerical Methods in Water Resources, Computational Mechanics Publications, Southampton, U.K., pp. 77-84.

[2] Arbogast, T., and Wheeler, M.F. (in press) "A characteristics-mixed finite element method for advection dominated transport problems", SIAM J. Numerical Analysis.

[3] Arbogast, T., Wheeler, M.F., and Yotov, I. (in preparation) "Mixed finite elements for elliptic problems with tensor coefficients as finite differences".

[4] Arbogast, T., Wheeler, M.F., and Yotov, I. (in preparation) "Mixed finite element methods on general geometry".

[5] Raviart, R.A., and Thomas, J.M. (1977) "A mixed finite element method for 2nd order elliptic problems", in Mathematical Aspects of the Finite Element Method, Lecture Notes in Math. 606, Springer-Verlag, New York, pp. 292–315.

[6] Russell, T.F., and Wheeler, M.F. (1983) "Finite element and finite difference methods for continuous flows in porous media", in Ewing, R.E. (ed.), The Mathematics of Reservoir Simulation, Frontiers in Applied Mathematics 1, Society for Industrial and Applied Mathematics, Philadelphia, Chapter II, pp. 35–106.

[7] Thomas, J.M. (1977) "Sur l'analyse numérique des méthodes d'éléments finis hybrides et mixtes", Thèse d'Etat, Université Pierre et Marie Curie.

[8] Weiser, A., and Wheeler, M.F. (1988) "On convergence of block-centered finite-differences for elliptic problems", SIAM J. Numerical Analysis 25, pp. 351–375.